

Implicit Neural Representation in Medical Imaging: A Comparative Survey

Amirali Molaei¹ Amirhossein Aminimehr¹ Armin Tavakoli¹ Amirhossein Kazerouni²
Bobby Azad³ Reza Azad⁴ Dorit Merhof^{5,6}

¹ School of Computer Engineering, Iran University of Science and Technology, Iran

² School of Electrical Engineering, Iran University of Science and Technology, Iran

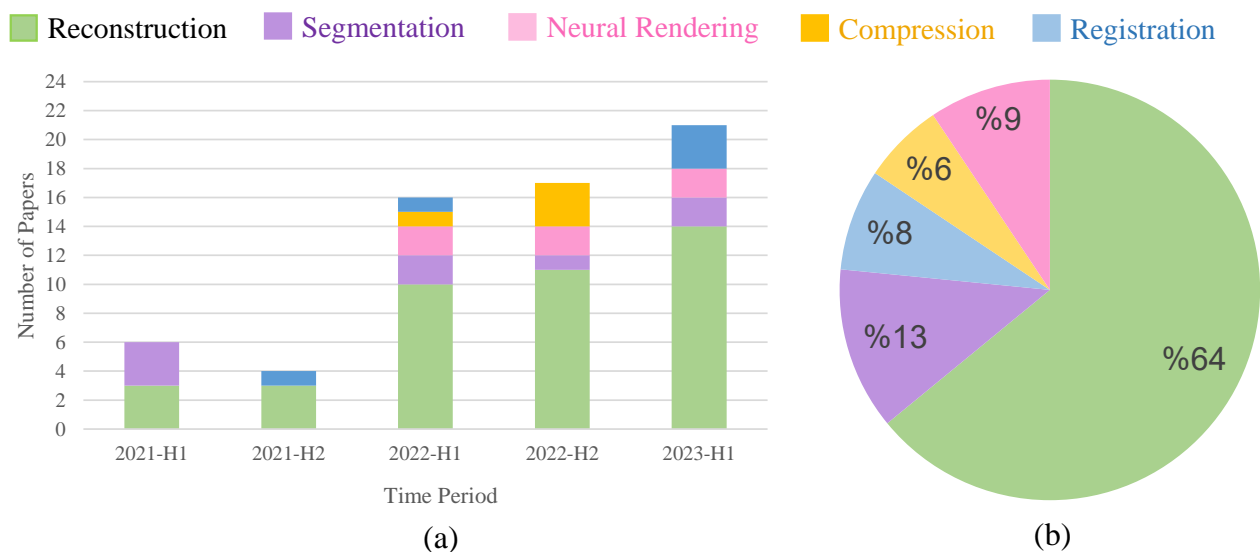
³ Department of Electrical Engineering and Computer Science, South Dakota State University, USA

⁴ Faculty of Electrical Engineering and Information Technology, RWTH Aachen University, Germany

⁵ Faculty of Informatics and Data Science, University of Regensburg, Germany

⁶ Fraunhofer Institute for Digital Medicine MEVIS, Bremen, Germany

{molaeiamirali, amirhossein477, rezazad68}@gmail.com, bobby.azad@jacks.sdstate.edu,
{amir_aminimehr, armin.tavakoli}@comp.iust.ac.ir, dorit.merhof@ur.de



[t] Figure 1: Chart (a) visually displays the relative proportions of published papers according to their application, and chart (b) illustrates the count of published papers based on INR design in medical tasks during different time periods (with "H" indicating the first or second half of the year). The assessment of the statistics is based on a sample of 64 research papers published during the years 2021 to 2023.

A. further discussion

The field of medical imaging has witnessed a remarkable upsurge in the utilization of implicit neural representation (INR) techniques, as evident from the exponential growth in research papers dedicated to this domain (Figure 1). This surge of interest in INR within the medical imaging community has resulted in a multitude of applications across diverse medical imaging scenarios. Recognizing the significance of INR and the influx of contributions in this realm, the time is ripe for a comprehensive survey of the existing literature. In the main part of our paper, we conducted an

all-encompassing survey aimed at providing a comprehensive overview of recent advancements in INR models within the field of medical imaging. Through an exhaustive analysis of the pertinent literature, we discovered that we are the pioneers in delivering comprehensive coverage of the implementation of INR models specifically tailored for the medical domain. By meticulously identifying and succinctly summarizing the pivotal findings and techniques employed in these models (refer to Table 1), we strive to not only provide invaluable insights but also forge novel research paths. Moreover, our intention is to ignite a renewed fervor within the vision community, encouraging them to capitalize on the

immense potential of INR models in the context of medical imaging.

References

- [1] Oliver JD Barrowclough, Georg Muntingh, Varatharajan Nainamalai, and Ivar Stangeby. Binary segmentation of medical images using implicit spline representations and deep learning. *Computer Aided Geometric Design*, 85:101972, 2021. [3](#)
- [2] Abril Corona-Figueroa, Jonathan Frawley, Sam Bond-Taylor, Sarath Bethapudi, Hubert PH Shum, and Chris G Willcocks. Mednerf: Medical neural radiance fields for reconstructing 3d-aware ct-projections from a single x-ray. In *2022 44th Annual International Conference of the IEEE Engineering in Medicine & Biology Society (EMBC)*, pages 3843–3848. IEEE, 2022. [3](#)
- [3] Yu Fang, Lanzhuju Mei, Changjian Li, Yuan Liu, Wenping Wang, Zhiming Cui, and Dinggang Shen. Snaf: Sparse-view cbct reconstruction with neural attenuation fields. *arXiv preprint arXiv:2211.17048*, 2022. [3](#)
- [4] Jia Gu, Fangzheng Tian, and Il-Seok Oh. Retinal vessel segmentation based on self-distillation and implicit neural representation. *Applied Intelligence*, pages 1–18, 2022. [3](#)
- [5] Albert W Reed, Hyojin Kim, Rushil Anirudh, K Aditya Mohan, Kyle Champley, Jingu Kang, and Suren Jayasuriya. Dynamic ct reconstruction from limited views with implicit neural representations and parametric motion fields. In *Proceedings of the IEEE/CVF International Conference on Computer Vision*, pages 2258–2268, 2021. [3](#)
- [6] Katja Schwarz, Yiyi Liao, Michael Niemeyer, and Andreas Geiger. Graf: Generative radiance fields for 3d-aware image synthesis. *Advances in Neural Information Processing Systems*, 33:20154–20166, 2020. [3](#)
- [7] Liyue Shen, John Pauly, and Lei Xing. Nerp: implicit neural representation learning with prior embedding for sparsely sampled image reconstruction. *IEEE Transactions on Neural Networks and Learning Systems*, 2022. [3](#)
- [8] Shanlin Sun, Kun Han, Deying Kong, Chenyu You, and Xiaohui Xie. Mirnf: Medical image registration via neural fields. *arXiv preprint arXiv:2206.03111*, 2022. [3](#)
- [9] Yu Sun, Jiaming Liu, Mingyang Xie, Brendt Wohlberg, and Ulugbek S Kamilov. Coil: Coordinate-based internal learning for imaging inverse problems. *arXiv preprint arXiv:2102.05181*, 2021. [3](#)
- [10] Yuehao Wang, Yonghao Long, Siu Hin Fan, and Qi Dou. Neural rendering for stereo 3d reconstruction of deformable tissues in robotic surgery. In *International Conference on Medical Image Computing and Computer-Assisted Intervention*, pages 431–441. Springer, 2022. [3](#)
- [11] David Wiesner, Julian Suk, Sven Dummer, David Svoboda, and Jelmer M Wolterink. Implicit neural representations for generative modeling of living cell shapes. In *International Conference on Medical Image Computing and Computer-Assisted Intervention*, pages 58–67. Springer, 2022. [3](#)
- [12] Jelmer M Wolterink, Jesse C Zwienenberg, and Christoph Brune. Implicit neural representations for deformable image registration. In *International Conference on Medical Imaging with Deep Learning*, pages 1349–1359. PMLR, 2022. [3](#)
- [13] Qing Wu, Yuwei Li, Yawen Sun, Yan Zhou, Hongjiang Wei, Jingyi Yu, and Yuyao Zhang. An arbitrary scale super-resolution approach for 3d mr images via implicit neural representation. *IEEE Journal of Biomedical and Health Informatics*, 27(2):1004–1015, 2022. [3](#)
- [14] Qing Wu, Yuwei Li, Lan Xu, Ruiming Feng, Hongjiang Wei, Qing Yang, Boliang Yu, Xiaozhao Liu, Jingyi Yu, and Yuyao Zhang. Irem: high-resolution magnetic resonance image reconstruction via implicit neural representation. In *Medical Image Computing and Computer Assisted Intervention—MICCAI 2021: 24th International Conference, Strasbourg, France, September 27–October 1, 2021, Proceedings, Part VI 24*, pages 65–74. Springer, 2021. [3](#)
- [15] Runzhao Yang. Tinc: Tree-structured implicit neural compression. In *Proceedings of the IEEE/CVF Conference on Computer Vision and Pattern Recognition*, pages 18517–18526, 2023. [3](#)
- [16] Runzhao Yang, Tingxiong Xiao, Yuxiao Cheng, Qianni Cao, Jinyuan Qu, Jinli Suo, and Qionghai Dai. Sci: A spectrum concentrated implicit neural compression for biomedical data. In *Proceedings of the AAAI Conference on Artificial Intelligence*, volume 37, pages 4774–4782, 2023. [3](#)
- [17] Hang Zhang, Rongguang Wang, Jinwei Zhang, Chao Li, Gufeng Yang, Pascal Spincemaille, Thanh Nguyen, and Yi Wang. Nerd: Neural representation of distribution for medical image segmentation. *arXiv preprint arXiv:2103.04020*, 2021. [3](#)

Table 1: A comparison of different proposed methods in different medical imaging task. The table is divided into different sections based on the imaging task, including Reconstruction, Segmentation, Neural Rendering, Compression, and Registration.

Application	Method	Input	Output	Activation Function	Modality	Highlight	Ref
Reconstruction	NeRP	(x, y, z)	Intensity	ReLU	MRI CT	Reconstructs high-quality CT and MRI images from sparsely sampled measurements by embedding a prior image from an earlier scan, training the network to learn the neural representation of the target image, and inferring the trained network to generate the final reconstructed image.	[7]
	DCTR	(x, y, z)	Linear Attenuation Coefficient	ReLU	CT	Calculating the loss between the new CT measurement and the measurement taken in the previous time step, then propagates the loss back to the MLP in order to remove noise from the new scan and reconstruct its CT image.	[5]
	IREM	(x, y, z)	Intensity	ReLU	MRI	Generates 3D MRI volumes by fitting implicit neural representations on sagittal, coronal, and axial planes of the brain to reconstruct the vacant voxels between them.	[14]
	ArSSR	(x, y, z) Image Embedding	Intensity	ReLU	MRI	represents the 3D brain MRI surface using high-resolution (HR) and low-resolution (LR) image pairs. The LR image is processed through task-specific super-resolution CNN to extract features, which are concatenated with the HR image coordinates. This concatenated input is then used by a decoder MLP to generate the 3D voxel intensity.	[13]
	INR-LCS	(x, y, z) τ (Temporal variable) z (latent code)	SDF	Sine	Fluorescent Microscopy	<ul style="list-style-type: none"> • Uses an MLP to represent the signed distance function (SDF) of evolving cell shapes at any point given its spatial coordinates (x, y, z), a temporal parameter (t), and a conditioning latent code that provides additional information and influences the generated cell shapes. • Can aid researchers in studying subjects such as cell division, migration, or modifications in cellular structures. 	[11]
	CoIL	(θ, l)	Response (r)	ReLU	CT	By utilizing the viewing angle θ and the spatial location l of the relevant detector on the sensor plane as inputs, an MLP learns a mapping to sensor responses (CT measurement) in order to represent the measurement field of the organ of interest.	[9]
Segmentation	BS-ISR	(x, y)	Spline Coefficient	ReLU	CT	Used a combination of INR and CNNs to model the segmentation boundary by mapping CT slice coordinates to spline coefficients.	[1]
	NeRD	(d_t, d_r, d_b, d_l)	(μ, Σ)	ReLU	MRI	Addressed the spatial invariance challenge caused by pooling and padding operations by using a pixel-wise 4D position vector (distance from the top, right, bottom, and left) as input to train an MLP representing pixel-wise distribution in order to generate the mean and covariance matrix of that pixel.	[17]
	Retinal INR	(x, y)	RGB Value	χ	Fundus Photography	An INR model enhances the retinal image resolution, while a Vision Transformer (ViT) conducts self-distillation on the original image to extract the key features. These features are utilized for the segmentation of retinal vessels, therefore aiding in the detection of ocular diseases.	[4]
Neural Rendering	MedNeRF	(x, y, z, θ, ϕ)	(RGB, σ)	ReLU	CT	Combines NeRF and a CNN (inspired by GRAF [6]) to generate CT projections from X-rays by training NeRF as the generator to output image patches and a CNN as the discriminator to refine NeRF outputs, enhancing image quality and addressing NeRF's struggles with complex scenes.	[2]
	Surgical Neural Rendering	(x, y, z, θ, ϕ)	(RGB, σ)	ReLU	Endoscopic imaging	NeRF-based rendering in robotic surgery that captures non-rigid deformations and reconstructs the 3D structures of the surgical scenes, from single-viewpoint stereo endoscopes. It handles occlusion caused by surgical instruments by utilizing a canonical radiance field and a time-dependent displacement field. The canonical field maps coordinates and viewing directions to colors and space occupancy, while the displacement field maps input space-time coordinates to displacement vectors.	[10]
	SNAF	(x, y, z)	Attenuation Coefficient	ReLU	CBCT	<ul style="list-style-type: none"> • Neural rendering is utilized as part of the CBCT reconstruction process to enhance the quality of the rendered CBCT images by learning neural attenuation fields using a multi-resolution hash table and employing volume rendering, high-quality CBCT images are generated from sparse 2D projections. • The deblurring network takes as input a rendered novel view from the learned neural attenuation field, along with its neighboring views to mitigate the blurring effect resulting from limited input projections. 	[3]
Compression	SCI	(x, y, z)	Compressed Representation	Sine	CT	<ul style="list-style-type: none"> • Mitigates INR's limitations on broad-spectrum data by introducing adaptive partitioning, which divides the data into blocks within INR's spectrum envelop and compresses each block using a funnel-shaped neural network architecture (wider beginning and narrower end) to capture its spectrum and characteristics, resulting in compressed data obtained through parameter optimization and serialization. • Their findings demonstrate that INR struggles to accurately represent data with a wide range of frequencies, impacting its fidelity in capturing diverse spectral components. 	[16]
	TINC	(x, y, z)	Compressed Representation	Sine	Phase-Contrast CT	Uses octree partitioning to enable visually similar blocks to share parameters within a tree-shaped neural network structure, enhancing representation compactness and resulting in a more efficient and concise architecture, achieved through an MLP-based implicit neural function representation of each equal-sized block of target data.	[15]
Registration	IDIR	(x, y, z)	Deformation Vector	Sine	CT	Leverages insights from differentiable rendering to demonstrate how an implicit deformable image registration model can be combined with regularization terms using automatic differentiation techniques. The use of periodic activation functions allows for higher-order derivatives, which facilitates more advanced regularization techniques and leads to improved control over deformations and enhanced accuracy in image registration.	[12]
	mimf	(x, y, z)	Displacement Vector Velocity Vector	Sine	MRI	A novel framework that combines optimization with deep neural networks for image registration. It utilizes neural fields to represent the transformation between pair of images, offering two methods for generating deformation fields. The optimal registration is achieved through parameters of neural field update via stochastic gradient descent. The paper also discusses ways to enhance model optimization.	[8]